J. Mol. Biol. (1998) **276**, 177–187

JMB

Solution Structure of the Glycosylated Second Type 2 Module of Fibronectin

Heinrich Sticht, Andrew R. Pickford, Jennifer R. Potts and Iain D. Campbell*

Department of Biochemistry University of Oxford, South Parks Road, Oxford, OX1 3QU UK

*Corresponding author

Fibronectin is an extracellular matrix glycoprotein that plays a role in a number of physiological processes involving cell adhesion and migration. The modules of the fibronectin monomer are organized into proteolytically resistant domains that in isolation retain their affinity for various ligands. The tertiary structure of the glycosylated second type 2 module (^{2}F2) from the gelatin-binding domain of fibronectin was determined by two-dimensional nuclear magnetic resonance spectroscopy and simulated annealing.

The structure is well defined with an overall fold typical of F2 modules, showing two double-stranded antiparallel β-sheets and a partially solvent-exposed hydrophobic cluster. An N-terminal β-sheet, that was not present in previously determined F2 module structures, may be important for defining the relative orientation of adjacent F2 modules in fibronectin. This is the first three-dimensional structure of a glycosylated module of fibronectin, and provides insight into the possible role of the glycosylation in protein stability, protease resistance and modulation of collagen binding.

Based on the structures of the isolated modules, models for the ^{1}F2^{2}F2 pair were generated by randomly changing the orientation of the linker peptide between the modules. The models suggest that the two putative collagen binding sites in the pair form discrete binding sites, rather than combining to form a single binding site.

Keywords: fibronectin; type 2 module; NMR; collagen; glycosylation

Introduction

Fibronectin is a large extracellular glycoprotein that exists as a soluble dimer in many body fluids, and as insoluble multimeric fibrils in the extracellular matrix. It plays a crucial role in many physiological processes such as wound healing, embryogenesis, haemostasis and thrombosis (for review see Hynes, 1990; Potts & Campbell, 1994, 1996). Numerous studies have provided evidence for an interaction between fibronectin and collagen within the extracellular matrix *in vivo* (reviewed by Hynes, 1990). *In vitro*, fibronectin binds to various types of isolated collagen α-chains (Guidry *et al.*, 1990), and denatured collagen (gelatin; Hahn & Yamada, 1979; Forastieri & Ingham, 1985).

The fibronectin monomer is composed almost entirely of three types of modules, F1, F2 and F3. The gelatin binding site is located within a 42 kDa proteolytic fragment with the modular structure ^{6}F1^{1}F2^{2}F2^{7}F1^{8}F1^{9}F1 (where ^{n}F*X* denotes the *n*th type *X* module in the protein). This gelatin-binding domain possesses three N-linked sugars (one on ^{2}F2 and two on ^{8}F1), the carbohydrate composition of which differ between different sources (Krusius *et al.*, 1985) and may modulate the protein's affinity for various ligands (Kottgen *et al.*, 1989). However, complete deglycosylation appears to have little or

Present address: H. Sticht, Lehrstuhl für Struktur und Chemie der Biopolymere, Universität Bayreuth, Universitätsstr. 30, D-95447 Bayreuth, Germany.

Abbreviations used: COSY, correlated spectroscopy; DQF-COSY, double-quantum-filtered COSY; F1, fibronectin type 1 module; F2, fibronectin type 2 module; ^{n}F*X*, *n*th type *X* module in fibronectin; GlcNAc, *N*-acetyl-glucosamine; $^{3}J_{HN\alpha}$, intra-residue NH-C$^{\alpha}$H coupling constant; $^{3}J_{\alpha\beta}$, intra-residue C$^{\alpha}$H-C$^{\alpha}$H coupling constant; MALDI, matrix assisted laser desorption/ionization; MD, molecular dynamics; MMP9, matrix metalloproteinase 9; NOE, nuclear Overhauser effect; PE-COSY, primitive exclusive COSY; rmsd, root-mean-square deviation; TOCSY, total correlation spectroscopy.

0022–2836/98/060177–11 $25.00/0/mb971528

no effect on the affinity for gelatin (Jones *et al.*, 1976; Dellanoy & Montreuil, 1989).

The exclusive location of the F2 modules in fibronectin to the gelatin-binding domain, and their presence in a range of other gelatin-binding proteins, such as the matrix metalloproteinases (MMPs) 2 and 9 and the bovine seminal fluid protein PDC-109, suggests that F2 modules are directly involved in gelatin binding. Furthermore, recombinant F2 modules from MMPs possess high affinity for gelatin (Banyai & Patthy, 1991; Collier *et al.*, 1992; Banyai *et al.*, 1994), whereas recombinant MMP2 lacking F2 modules does not bind gelatin (Murphy *et al.*, 1994; Allan *et al.*, 1995). However, the ability of each of the ^{6}F1^{1}F2, ^{2}F2^{7}F1 and ^{8}F1^{9}F1 module pairs from fibronectin to bind gelatin, demonstrates that F1 modules may also be involved (Ingham *et al.*, 1989; Litvinovich *et al.*, 1991).

Solution structures of the F2 modules PDC-109b from PDC-109 (Constantine *et al.*, 1991, 1992), and ^{1}F2 from fibronectin (Pickford *et al.*, 1997) have been determined previously by NMR spectroscopy. Both proteins contain two double-stranded antiparallel β-sheets, oriented almost perpendicular to each other, which enclose a cluster of conserved aromatic amino acid residues, some of which form an exposed hydrophobic surface which may play a role in ligand binding (Constantine *et al.*, 1992; Pickford *et al.*, 1997). However, in comparison to PDC-109b, ^{1}F2 has an N-terminal extension of approximately 15 residues that folds back along the C-terminal β-sheet, bringing the N and C termini into close proximity (Pickford *et al.*, 1997). This topology might allow interactions between non-contiguous modules within the gelatin-binding domain.

Here we describe the determination of the solution structure of ^{2}F2 with a single N-linked N-acetylglucosamine (GlcNAc). Similar to ^{1}F2, ^{2}F2 has an N-terminal extension compared with PDC-109b. The aim of this work was to determine if the close proximity of the N and C termini observed in ^{1}F2 is conserved in ^{2}F2, and then build a model of the ^{1}F2^{2}F2 pair. The conformation of the sugar and the effect of glycosylation on the three-dimensional structure of ^{2}F2 is also assessed.

Results and discussion

Protein expression

The glycosated ^{2}F2 was produced by recombinant expression from the methylotrophic yeast *Pichia pastoris* as described in Materials and Methods. Electrospray and MALDI mass spectrometry of the ^{2}F2 module revealed masses of 7051.5 and 7051.0 Da, respectively, approximately 156 Da greater than expected for the 59-residue module with a single GlcNAc. N-terminal sequence analysis revealed this to be due to the presence of an additional arginine residue at the N terminus, which probably arose from inaccurate cleavage of the α-factor signal sequence by the endogenous *P. pastoris* processing enzyme KEX2. Both mass spectrometric techniques proved a uniform product which was more than 95% pure.

Resonance assignments and secondary structure of ^{2}F2

Sequence-specific resonance assignments were performed according to standard procedures (Wüthrich, 1986) using the set of spectra acquired at 25°C. In the case of ambiguities caused by peak overlap or coincidence with the water signal, spectra acquired at 37°C were used for assignment. The complete resonance assignment of all backbone and of most side-chain protons was obtained and is available as supplementary material.

The resonances of the Arg − 1 residue could be assigned, but this residue was not taken into account in the final structure calculations, since two independent initial calculations with and without this residue proved to be indistinguishable in terms of energy and structure.

The Phe17($C^{\alpha}H$) and Pro18($C^{\alpha}H$) resonances of ^{2}F2 were coincident at both 25 and 37°C. Therefore, it was not possible to establish the isomeric form of Pro18 unambiguously from the NMR spectra. However, the equivalent residue in the structures of PDC-109b and ^{1}F2 is a *cis*-proline (Constantine *et al.*, 1991; Pickford *et al.*, 1997), so it is likely that this invariant residue adopts a *cis*-conformation in all F2 modules. Furthermore, structure calculations of ^{2}F2 performed with Pro18 in a *cis* conformation resulted in a 15 to 20% lower target function energy than for a *trans* conformation.

Elements of secondary structure were identified from the intensity of the sequential NOEs, the $^{3}J_{HN\alpha}$ coupling constants, slowly exchanging amide protons and chemical shift index (Wishart *et al.*, 1992; Figure 1). According to these criteria, four extended strands were identified which, from the pattern of long-range NOEs and slowly exchanging amide protons, form two double-stranded antiparallel β-sheets (Figure 2).

Long-range NOEs typical of a β-sheet were also observed for residues 4 to 6 and 12 to 15 (Figure 2), although from the analysis of the $^{3}J_{HN\alpha}$ coupling constants, the amide proton exchange data and the chemical shift index (Figure 1), this sheet appears to be less stable than those above. Helix-typical $\{i\}C^{\alpha}H$-$\{i+3\}NH$, $\{C^{\alpha}H$-$\{i+3\}C^{\beta}H$ and $\{i\}C^{\alpha}H$-$\{i+4\}NH$ NOEs were observed for residues 47 to 51, suggesting the presence of a single helical turn (Figure 1).

Tertiary structure of ^{2}F2 and comparison with ^{1}F2

The calculation of the final structures was based on 583 distance restraints, 43 dihedral angle restraints and 30 hydrogen bond restraints which are summarized in Table 1. The distribution of the

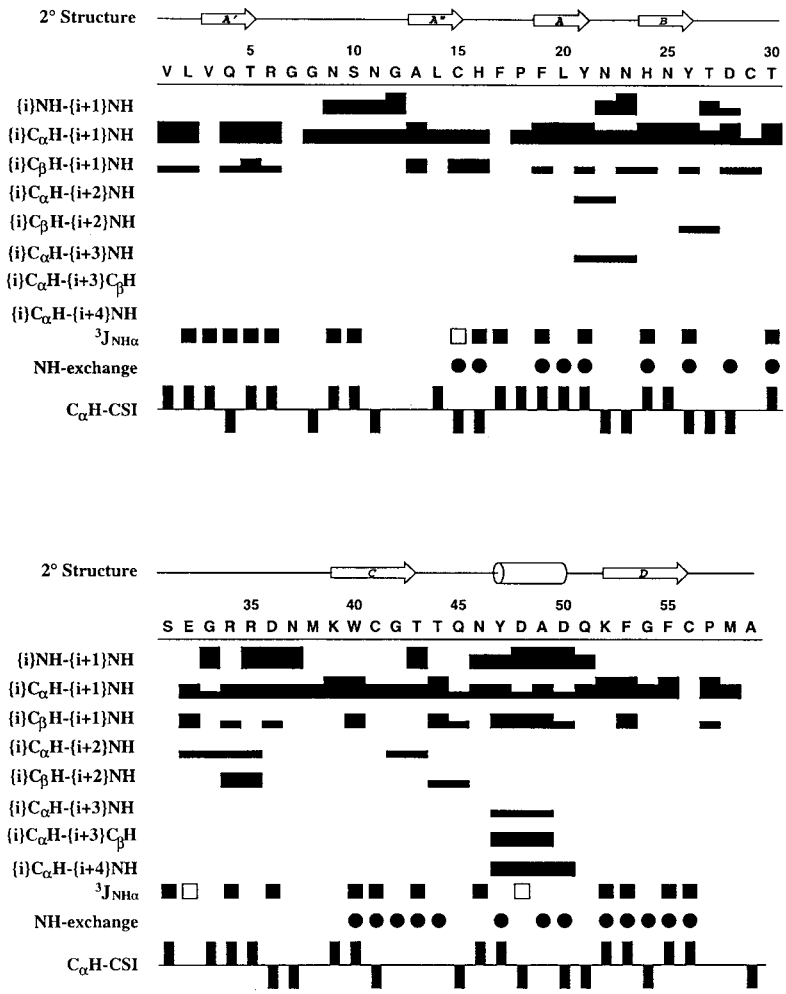

Figure 1. Secondary structure of the ²F2 module: summary of sequential and medium-range NOEs, slowly exchanging amide protons, vicinal backbone NH-C$^{\alpha}$H coupling constants ($^3J_{NH\alpha}$) and chemical shifts indices (C$^{\alpha}$H-CSI; Wishart *et al.*, 1992). The relative strengths of the NOEs, categorized as strong, medium or weak, by cross-peak intensity, are indicated by the width of the horizontal bars. Values of $^3J_{HN\alpha}$ >8 Hz or <6 Hz are denoted by filled and open squares, respectively. Backbone amide protons that were observable more than 16 hours after transfer of the protein sample from H_2O to ^2H_2O are marked by filled circles. Positive or negative chemical shift indices are denoted by filled rectangles above or below the axis, respectively. Regions of β-sheet are typified by positive chemical shift indices, and α-helix by negative (Wishart *et al.*, 1992). The secondary structure assignments (2°) are depicted above the molecule sequence.

NOEs as a function of the residue number is given in Figure 3(a).

In general, the structure of ²F2 is well defined with backbone root-mean-square deviations (rmsds) of less than 0.8 Å and ϕ and ψ angle order parameters (Hyberts *et al.*, 1992) greater than 0.9 for the majority of the protein backbone. Higher backbone rmsds and lower angle order parameters are found for the N and C-terminal residues and for residues 35 to 38 (Figure 3(b)). The orientations of the side-chains is particularly well-defined for the aromatic residues in ²F2 (Figure 4).

According to PROCHECK (Laskowski *et al.*, 1993) analysis of the family of 80 structures, all residues show energetically favourable backbone conformations: 56% of the residues are found in the most favoured regions and 44% in the allowed regions of the Ramachandran plot (data not shown).

Figure 5 shows a schematic representation of the minimized average structure of ²F2 with a short α-helix and three antiparallel β-sheets, which partly enclose a cluster of aromatic residues. Ring-current effects from these residues are the likely causes of some unusual proton chemical shifts for the module, e.g. Thr30(C$^{\gamma}$H$_3$) 0.09 ppm and Gly42(NH) 3.63 ppm. The topology is similar to that of ¹F2 (Pickford *et al.*, 1997) and for the regions of common secondary structure, the backbone rmsd is 0.82 Å between the minimized average structures of both modules (Figure 6).

In both fibronectin F2 modules, the distance between the N and C termini is short (approximately 7.0 Å for C$^{\alpha}$-carbon atoms of residues 4 and 57), but relative to ¹F2, the N terminus of ²F2 is shifted towards residues Gly12 to Cys15, forming a double-stranded antiparallel β-sheet (Figure 2). The backbone-backbone interactions observed between the N and C-terminal strands in ¹F2 (Pickford *et al.*, 1997) are replaced by numerous hydrophobic interactions and hydrogen bonds between the side-chains of the N and C-terminal regions in ²F2. The observed slow exchange of the amide protons of Phe53 and Phe55 probably results from hydrogen bonds to the side-chains of Asn9 and Thr5, respectively. The apparent greater flexibility of the N-terminal region in ¹F2 (NH_2-AVT...) relative to that of ²F2 (NH_2-VLV...) may arise from differences in their hydrophobicity. In ²F2, Leu2 and Val3 in the N-terminal region show hydrophobic contacts to residues Leu14, Pro57 and Met58.

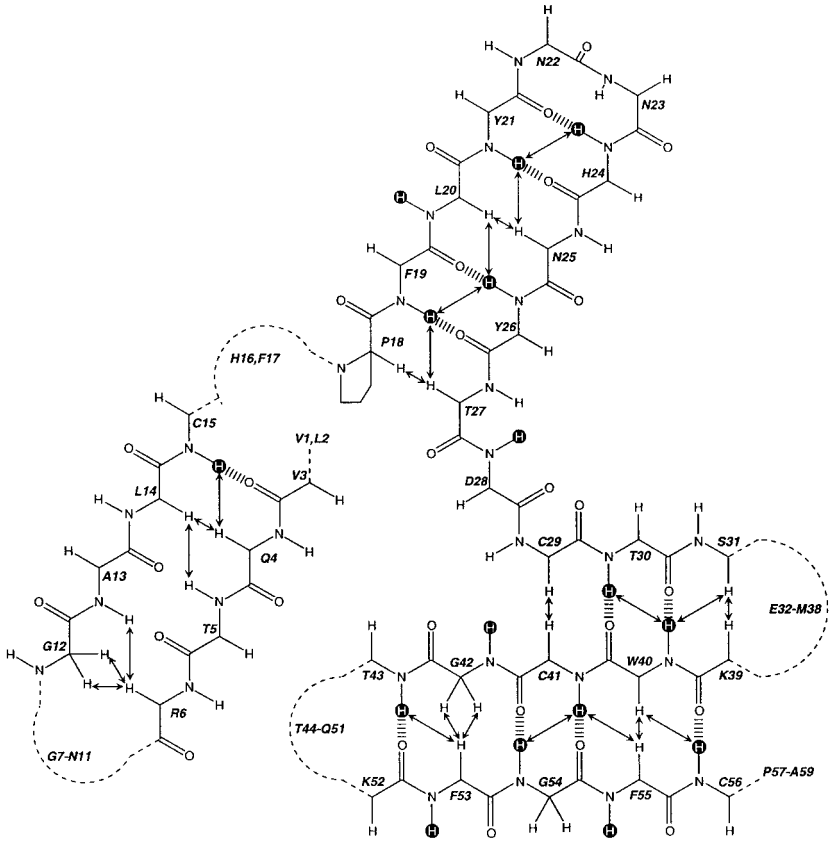

Figure 2. Schematic representation of the extended regions of ^{2}F2. Inter-strand NOEs are depicted by double-headed arrows, slowly exchanging backbone amide protons by filled circles, and hydrogen bonds by stacked bars.

Table 1. Structural statistics for the family of 80 ^{2}F2 structures

Rmsd (±s.d.) from experimental distance restraints (Å)[a]	
All NOE constraints (583)	0.020 ± 0.003
Intra-residue $\{\|i-j\|=0\}$ (208)	0.021 ± 0.003
Sequential $\{\|i-j\|=1\}$ (146)	0.022 ± 0.002
Short range $\{1>\|i-j<5\}$ (47)	0.027 ± 0.003
Long range $\{\|i-j\|>4\}$ (182)	0.014 ± 0.001
Hydrogen bonds (30)	0.012 ± 0.001
Rmsd (± s.d.) from experimental torsion angle restraints (°)[a]	
ϕ angles (28)	0.122 ± 0.003
χ^1 angles (11)	0.141 ± 0.004
Sugar dihedrals (4)	0.179 ± 0.008
Rmsd (± s.d.) from idealized covalent geometry	
Bond lengths (Å)	0.03 ± 0.000
Angles (°)	0.552 ± 0.012
Impropers (°)	0.591 ± 0.066
X-PLOR potential energies ± s.d. (kcal mol^{-1})	
E_{total}	128.3 ± 7.2
E_{repel}	22.8 ± 2.1
E_{NOE}	13.0 ± 3.3
E_{bond}	5.8 ± 0.5
E_{angle}	75.0 ± 3.0
$E_{improper}$	11.1 ± 0.8
$E_{dihedral}$	0.6 ± 0.0
$E_{L\text{-}J}$	−111.3 ± 10.4
Rmsd of cartesian coordinates (Å)[c]	
Backbone N, C$^\alpha$ and C (residues 2–57)	0.55 ± 0.21
All heavy atoms (residues 2–57)	0.96 ± 0.35
GlcNAc (heavy atoms)	1.19 ± 0.45

[a] The number of each type of constraint is shown in parentheses. None of the 80 structures showed distance violations of more than 0.3 Å or dihedral angle violations of more than 2.0°. No distance or dihedral angle restraints were consistently violated more than 0.1 Å or 1.0°, respectively.

[b] E_{total}, total energy; E_{repel}, repulsive energy term; E_{NOE}, effective NOE energy term. The Lennard-Jones energy term ($E_{L\text{-}J}$) was not included in the target function. It was calculated using the full CHARMM potential function (Brooks *et al.*, 1983) without further minimization.

[c] Rmsd values result from a superposition on the N, C$^\alpha$ and C atoms of the protein backbone, and were calculated by averaging the individual rmsds between the average structure and each member of the family (Morton *et al.*, 1996).

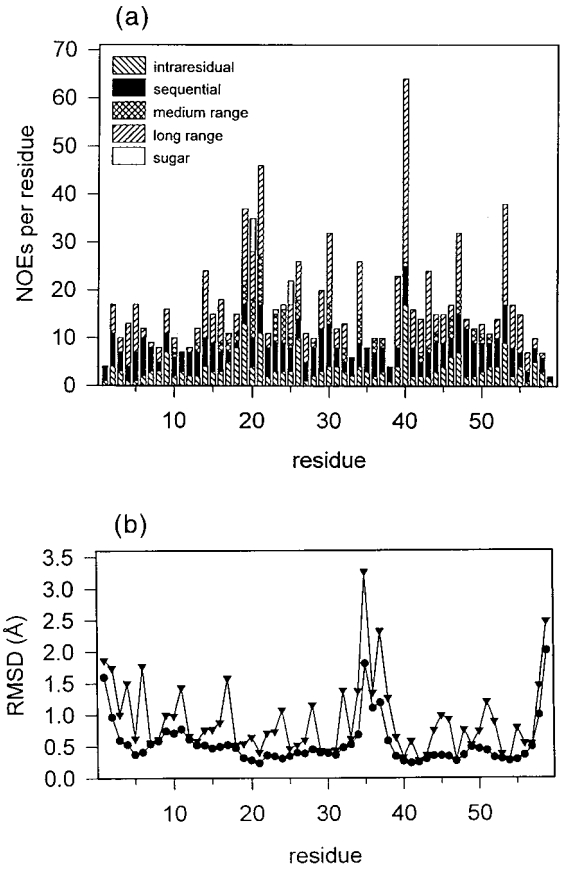

Figure 3. Correlation between the number of NOE restraints and the rmsd values of the resulting structures. a, Number of NOEs per residue used in the final round of the structure calculation. NOEs are grouped into intra-residue, sequential ($i-j=1$), medium-range ($i-j<5$) and long-range ($i-j \geqslant 5$). NOEs between protein and carbohydrate are listed separately. b, Average rmsd per residue between the 80 final structures. The rmsd values for the backbone heavy atoms and for all heavy atoms are represented by circles and triangles, respectively.

Residues Phe19 to Tyr21 and His24 to Tyr26 form an antiparallel β-sheet and the strands are connected by a type I′ β-turn. Slight deviations from an ideal sheet geometry are observed for residues 20 and 25, allowing tight interactions with the GlcNAc residue. This distortion is consistent with the observation that residues 20 and 25 show $^3J_{HN\alpha}$ coupling constants of less than 8.0 Hz (Figure 1). A comparison with the homologous β-sheet in ^{1}F2 reveals that the global fold of this region is not significantly affected by the glycosylation.

Residues Lys39 to Thr43 and Lys52 to Cys56 form a double-stranded antiparallel β-sheet. Despite the presence of two glycine residues, the geometry of the β-sheet is well defined. An additional extended region, which comprises residues Thr30 and Ser31, is too short to be considered as a regular β-strand. These three extended regions are connected by two loops, Glu32 to Met38 and Thr44 to Gln51.

As in ^{1}F2 (Pickford *et al.*, 1997) the loop from Glu32 to Met38 was poorly defined by the NMR data suggesting that a conformationally dynamic B-C loop may be a characteristic of F2 modules. Residues Tyr47 to Gln51 form a single helical turn in ^{2}F2 which may be stabilized by the network of hydrogen bonds involving side-chains of the highly conserved residues Asn46, Asp48 and Asp50 and the backbone amide protons of Ala49, Asn23 and Asn46, respectively. The requirement for Asn46 and Asp50 for gelatin-binding activity of the F2 module has previously been shown by alanine-scanning mutagenesis of MMP9-^{2}F2 (Collier *et al.*, 1992). No homologous helix was detected in ^{1}F2, due possibly to the substitution of Asp48 in ^{2}F2 by Glu. At pH 4.5 (the conditions of the structural investigations), Asp48 in ^{2}F2 is likely to have a greater degree of ionization than Glu48 in ^{1}F2, leading to an enhanced helix stabilization in the former.

As in both PDC-109b and ^{1}F2, many of the highly conserved aromatic residues in ^{2}F2 are clustered on one face of the module, forming a solvent-exposed hydrophobic surface (Figure 5). A depression in this surface, at the bottom of which lies the invariant core tryptophan residue (Trp40), may bind non-polar residues such as those in the fibronectin-binding site of collagen α1(I) (Pickford *et al.*, 1997). The resonances of the equivalent tryptophan residue in PDC-109b were the most sensitive to the binding of leucine- and isoleucine-analogues to the module (Constantine *et al.*, 1992).

Structure of the carbohydrate

The resonances of the Asn25-linked GlcNAc sugar in ^{2}F2 were assigned by identification of through-bond couplings starting from Asn25($N^\delta H$), and by through-space couplings in the case of the acetyl group (Ac-CH_3). Two spin-systems of differing intensities were identified for GlcNAc, suggesting that the sugar moiety exists in two discrete forms. Analysis of the corresponding cross-peak intensities of the two systems revealed that the two forms were present in a ratio of approximately 10:1. Minor species have previously been reported in other studies of N-glycosylated peptides (Kessler *et al.*, 1991).

A full analysis of the Asn25 side-chain conformation was impeded by spectral overlap of the $C^\alpha H$-$C^\beta H$ crosspeaks with other resonances. Therefore, no restraints were deduced for the χ^1 and χ^2 angles of Asn25. However, for three other angles of the glycosidic linkage, restraints for the structure calculation could be derived on the basis of the NMR spectroscopic data. A ^3J($N^\delta H$(Asn25)-C_1H(GlcNAc)) coupling constant of 8.6 Hz, in conjunction with the NOE pattern, indicates that the C_1H-C_1-N^δ-$N^\delta H$ angle is close to 180° (Davis *et al.*, 1994). For the C^β-C^γ-N^δ-C_1 angle a *trans* conformation was deduced from the presence of strong

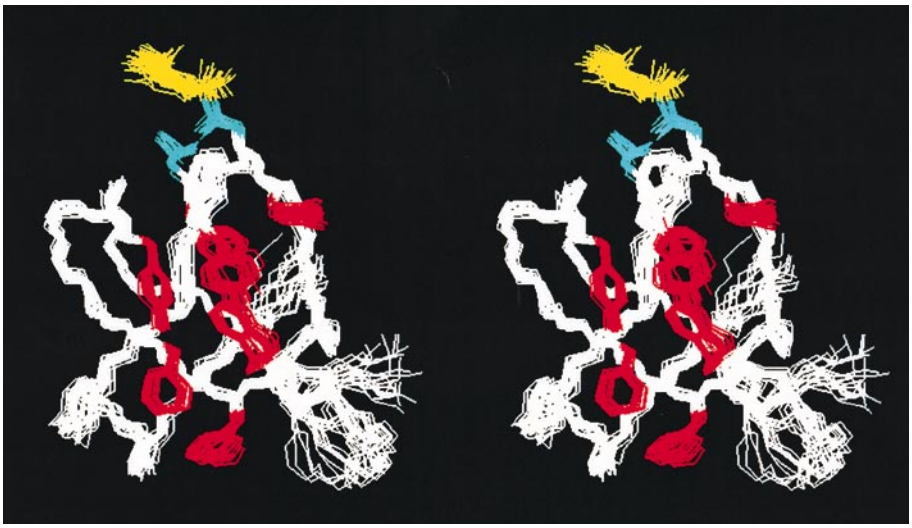

Figure 4. Stereoview showing a superimposition of the 20 lowest-energy structures of the ^{2}F2 module. The backbone heavy atoms (N, C^α and C) are shown in white with the side-chains of the highly conserved aromatic residues (Phe19, Tyr21, Tyr26, Trp40, Tyr47, Phe53 and Phe55) in red. The GlcNAc sugar is coloured yellow, and the residues with which it interacts (Leu20 and Asn25) are coloured cyan. This Figure was prepared using the program INSIGHT 2.3 (Biosym Technologies).

NOEs between the $N^\delta H$ and the two $C^\beta Hs$ of Asn25, and the lack of $C^\beta H$(Asn25)-C_1H(GlcNAc) NOEs. The conformation of the N-glycosidic linkage deduced from our NMR data is highly similar to that found in previous NMR studies (Wormald *et al.*, 1991; Davis *et al.*, 1994). The $^3J(C_1H\text{-}C_2H)$ coupling constant of the major conformation was measured as 9.7 Hz, consistent with a β-anomeric conformation, the most frequently observed anomer for N-linked GlcNAc sugars in solution (Vliegenthart *et al.*, 1983; Fletcher *et al.*, 1994).

The orientation of the β-anomeric GlcNAc attached to Asn25 is well defined in the family of calculated structures (Figure 4), with a similar conformation of the N-glycosidic linkage to that in previous NMR studies (Wormald *et al.*, 1991; Davis *et al.*, 1994). The GlcNAc conformation is stabilized by hydrophobic contacts between the acetyl group and Leu20, and by a hydrogen bond between the acetyl oxygen and the side-chain amide proton of

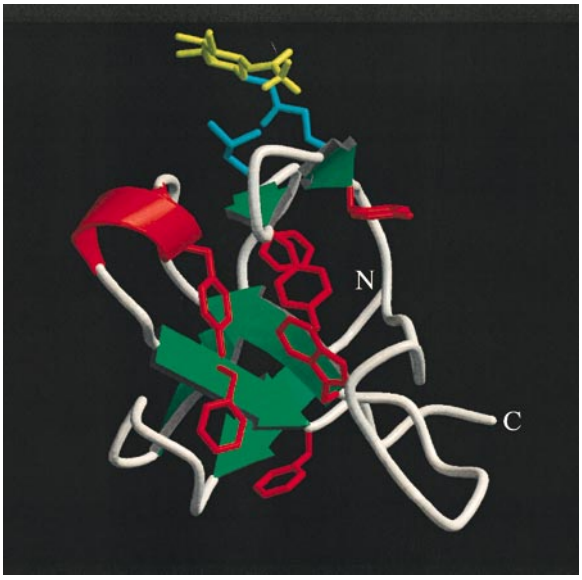

Figure 5. Schematic representation of the ^{2}F2 structure, showing the three β-sheets in green and a single turn of α-helix in red. The module orientation and the colour scheme for side-chains are as for Figure 4. This Figure was prepared using the programs MOLSCRIPT (Kraulis, 1991) and Raster3D (Bacon & Anderson, 1988; Merritt & Murphy, 1994).

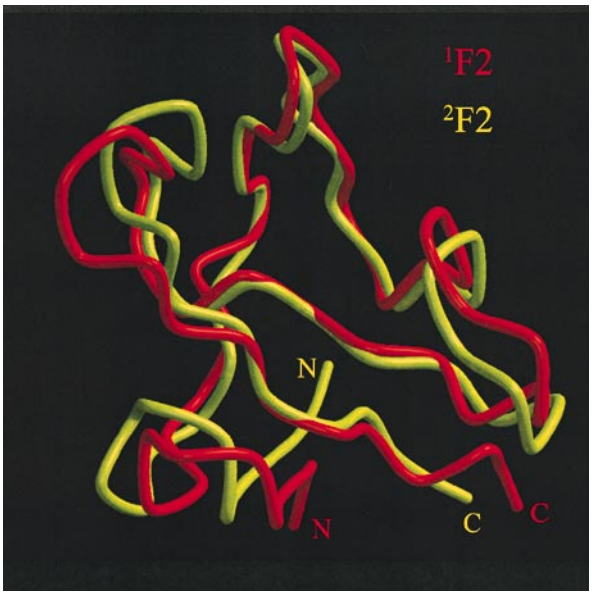

Figure 6. Comparison of the folds of the ^{1}F2 (red) and the ^{2}F2 (yellow) modules of fibronectin. The modules are superimposed over the backbone heavy atoms (N, C^α and C) of their common secondary structure elements. The ^{2}F2 module has been rotated by 25° relative to Figure 4 and 5. This Figure was prepared using the programs MOLSCRIPT (Kraulis, 1991) and Raster3D (Bacon & Anderson, 1988; Merritt & Murphy, 1994).

Asn25. These interactions may be responsible for the deviations from ideal β-sheet geometry observed for Leu20 and Asn25, each of which have $^3J_{HN\alpha}$ coupling constants of less than 8 Hz. Previous crystallographic and NMR studies have revealed similar hydrophobic contacts (Imberty *et al.*, 1993; Fletcher *et al.*, 1994; Wyss *et al.*, 1995) and hydrogen bonds (Imberty & Pérez, 1995) in other glycoproteins.

For the unrestrained C_2H-C_2-N_2-N_2H dihedral angle a range of 180 (±40)° is found in the calculated structures, which is in good agreement with the observed value of 8.0 Hz for $^3J(C_2H\text{-}N_2H)$. All torsion angles of the sugar are in the same range as the values reported from the analysis of crystal structures of other glycoproteins (Imberty & Pérez, 1995).

The relative inaccessibility of the N-glycosidic linkage due to carbohydrate-polypeptide interactions may explain the observed resistance of ^{2}F2 to deglycosylation by endoglycosidase F (Ingham *et al.*, 1995). Steric effects in interactions of fully glycosylated ^{2}F2 may confer proteolytic resistance to the gelatin-binding domain (Bernard *et al.*, 1982). Enhanced rigidity of a protein backbone by glycosylation was observed in previous NMR studies (Wormald *et al.*, 1991; Davis *et al.*, 1994).

The position and orientation of the GlcNAc (Figures 4 and 5) suggests that glycosylation would not directly interfere with ligand binding to the aromatic cluster of ^{2}F2. This is consistent with the observation that deglycosylation has no effect on the gelatin-binding activity of plasma fibronectin fragments (Jones *et al.*, 1976; Dellannoy & Montreuil, 1989). The reduced gelatin-binding activity of polylactosamine-containing placental fibronectin fragments (Zhu & Laine, 1985; Zhu *et al.*, 1990) may be due to steric hindrance of the binding site by these larger polar saccharides (Zhu & Laine, 1985). Alternatively, the polylactosamine chains may disrupt essential interactions with other modules, or hinder the binding of gelatin to other regions, e.g. the ^{6}F1^{1}F2 or ^{8}F1^{9}F1 module pairs. The fact that different glycoforms of a protein may display quite different orientations of the oligosaccharides with respect to the polypeptide has been reported previously for the Fc fragment of IgG (Deisenhofer, 1981; Malhotra *et al.*, 1995).

Models of the ^{1}F2^{2}F2 module pair of fibronectin

The ligand-binding properties of several fragments of the gelatin-binding domain have been studied by a number of groups and yet a fully functional binding site has not been localised exclusively to a single module. It seems likely, therefore, that the relative orientation of adjacent modules is important for the presentation of an optimal binding surface. A previous study used the PDC-109b F2 module structure to create a model of the F2 module triplet from MMP2 (Banyai *et al.*, 1996). However, PDC-109b lacks an N-terminal extension which is present in F2 modules from fibronectin, MMP2 and MMP9. Thus, we have modelled the structure of the ^{1}F2^{2}F2 module pair from fibronectin using the solution structures of ^{1}F2 (Pickford *et al.*, 1997) and ^{2}F2.

A total of 300,000 ^{1}F2^{2}F2 module pair structures with randomized inter-module backbone dihedral angles were screened, and 1087 of these structures were found to have favourable non-covalent interactions. All of these resulting structures have a similar overall location of the ^{2}F2 module relative to the ^{1}F2 module, but differ in their relative orientations.

No single structure exhibited a significantly lower energy than all the others. Possible explanations for this finding are the imperfection of the force field used and the absence of the neighbouring F1 modules in the modelling procedure, that occupy a part of the putative contact interfaces. Therefore, it was not possible to deduce the relative module orientation unambiguously. Nevertheless, there are two consistent features with important implications for the structure and function of the gelatin-binding domain.

First, in all analyzed structures a minimum distance of 14.2 Å is observed between the core tryptophan residues of the two F2 modules, suggesting that, in native fibronectin, the two hydrophobic pockets, which have been proposed to be involved in ligand binding, form discrete binding sites. This is in contrast to the recent model of the F2 module triplet from MMP2, created using the shorter PDC-109b structure, in which the three F2 modules are arranged with their hydrophobic pockets in close proximity to from a single binding site for a non-polar ligand (Banyai *et al.*, 1996).

Second, the distance between the N and C termini of approximately 20 Å (C^α(Gln4)-C^α(Pro117)) in all models is sufficiently short that it may allow the direct interactions between the non-contiguous ^{6}F1 and ^{7}F1 modules that have been proposed on the basis of thermodynamic studies (Litvinovich *et al.*, 1991).

The expression of the ^{1}F2^{2}F2 pair is currently underway in this laboratory in preparation for structural studies; its completion will allow the accuracy of the modelling strategy to be assessed, and may also indicate how the procedure could be improved. Although it is an ambitious goal, the ability to model module pairs or larger fragments from the solution structures of single modules would be invaluable to the understanding of the structure and function of fibronectin and of mosaic proteins in general.

Materials and Methods

Protein expression and purification

The 59-residue ^{2}F2 module, corresponding to residues 375 to 433 of mature human fibronectin was produced by recombinant expression from the methylotrophic yeast *P. pastoris* in an analogous fashion to that described

previously for the ^{1}F2 module (Pickford *et al.*, 1997). Before the final purification step, the high mannose sugar on the module was trimmed using endoglycosidase H_f (New England Biolabs) leaving a single N-acetylglucosamine (GlcNAc) attached to residue Asn25. The identity and purity of the recombinant ^{2}F2 was assessed by electrospray and MALDI mass spectrometry, and by N-terminal sequence analysis.

NMR spectroscopy

The sample for NMR spectroscopy contained approximately 2.5 mM protein in 0.5 ml $H_2O/^2H_2O$ (9 : 1, v/v, pH 4.5) or ^2H_2O (99.994 atom %). All NMR experiments were carried out at 500 MHz (^{1}H frequency) on home-built spectrometers consisting of Oxford Instruments 11.7 Tesla magnets operated by GE 1280 computers. Sets of spectra were collected at 25°C and 37°C, consisting of the following two-dimensional NMR experiments: DQF-COSY (Rance *et al.*, 1983), scuba-COSY (Brown *et al.*, 1988) and PE-COSY (Mueller, 1987), TOCSY (61 ms mixing time; Davis & Bax, 1985) and NOESY (150 ms mixing time; Kumar *et al.*, 1980). Slowly exchanging amide protons were identified from a series of short (approximately eight hour) TOCSY spectra collected after redissolving the lyophilized sample in ^2H_2O.

All experiments were acquired with 2048 complex points in t_2 and 400 to 640 complex points in t_1 and a sweep width of 8000 Hz in both dimensions. The States-time proportional phase incrementation method (Marion *et al.*, 1989) was used for acquisition in t_1.

Data processing was performed using the FELIX 2.3 software package (Hare Research Inc.) on Sun workstations. For all NOESY and TOCSY experiments a Lorentz-Gaussian multiplication (LB = −15 Hz; GB = 0.15) and a 70° phase-shifted squared sine-bell window function were applied prior to Fourier transformation in t_2 and t_1, respectively. DQF-COSY, scuba-COSY and PE-COSY spectra were processed using an unshifted sine-bell window function in both time domains.

NOE cross-peaks were categorized as ''strong'', ''medium'' or ''weak'' according to a calibration against the cross-peak intensity of the δ and ε protons of the aromatic rings and converted into upper limit distance constraints of 2.7, 3.3 and 5.0 Å, respectively (Eberle *et al.*, 1991). For distances involving either methylene protons without stereospecific assignments or methyl protons, $<r^{-6}>^{-1/6}$ averaged distances were used (as this quantity can be related directly to the experimental NOE; Brünger *et al.*, 1986). The $^3J_{HN\alpha}$ coupling constants were extracted from ω_2 cross-sections of a scuba-COSY spectrum that was processed to a digital resolution of 1.95 Hz/point as previously described (Williams *et al.*, 1993). In order to obtain the $^3J_{\alpha\beta}$ coupling constants, the frequency region around the corresponding cross-peak was extracted from the PE-COSY, inverse Fourier-transformed, zero-filled, and Fourier-transformed again. Final processing resulted in a digital resolution of 0.45 Hz/point in ω_2.

Experimental restraints for the structure calculations

A total of 656 experimental restraints were used for the structure calculations, with only unambiguous distance restraints included in the initial rounds of calculation. Additional distance restraints and 28 ϕ and 11 χ^1 dihedral angle restraints were included in several rounds of structure calculation after inspection of the initial structures, as described previously (Morton *et al.*, 1996; Pickford *et al.*, 1997). Restraints for χ^1 angles were only used if both the pattern of intra-residual NH-C^βH and C^αH-C^βH NOEs and the $^3J_{\alpha\beta}$ coupling constant pointed out one single value for χ^1.

One NOE distance restraint ($d_{ss} = 2.02(\pm 0.10)$Å) was added for each of the two disulphide bonds. Hydrogen bond restraints were introduced in the final round of the calculation if three criteria were met: a slow exchange of the corresponding amide proton, a N-H···O distance <2.3 Å and an O···H-N angle >120° in at least 70% of the unrestrained structures. For each hydrogen bond two distance restraints were introduced into the calculation: $d_{HN\text{-}O} = 1.7$ to 2.3 Å, $d_{N\text{-}O} = 2.4$ to 3.3 Å (Kraulis *et al.*, 1989).

The template structure of the Asn25-linked GlcNAc was obtained from the X-PLOR topology and parameter library for hetero compounds, with hydrogen atom positions and the covalent bond to Asn 25 added according to the geometry of the NAG model in the ''param3.cho'' parameter file (Weis *et al.*, 1990) that is supplied with the X-PLOR program package (Brünger, 1993). In order to obtain a correct local geometry during the high-temperature phase of the simulated annealing, all force constants were increased, matching the values of the ''parallhdg.pro'' force field of X-PLOR. A $^4C_1$ ring (''chair'') conformation was assumed, since this is usually observed for GlcNAc residues (Imberty & Pérez, 1995). In addition to the chair conformation, the C_1H-C_1-N^δ-N^δH, the C^β-C^γ-N^δ-C_1 and the C_1H-C_1-C_2-C_2H angle of the glycosidic linkage were restrained on the basis of the observed NOE pattern and coupling constants. For each of these dihedral angle restraints a deviation of ±30° from the equilibrium value was allowed without penalty.

Structure calculations and analysis

All structures were calculated using a modified *ab initio* simulated annealing protocol with an extended version of X-PLOR 3.1 (Brünger, 1993). The calculation strategy was similar to those described previously (Kharrat *et al.*, 1995; Kemmink *et al.*, 1996), including floating assignment of prochiral groups (Holak *et al.*, 1989) and a reduced presentation for non-bonded interactions for part of the calculation (Nilges, 1993) to increase efficiency.

Each round of the structure calculation started from templates with random backbone torsion angles. During all stages of the simulation the temperature was maintained by coupling to a heat bath (Berendsen *et al.*, 1984) with a coupling frequency of 10 ps^{-1}. In the conformational search phase 40 ps of MD were simulated at 2000 K, using a 2 fs timestep. In this stage of the calculation, the non-bonded interactions were only computed between C^α atoms and one carbon of each side-chain, using van der Waals radii of 2.25 Å (Nilges, 1993; Kharrat *et al.*, 1995). The refinement comprised a two-phase cooling procedure treating the non-bonded interactions between all atoms explicitly. In the first stage the system was cooled from 2000 K to 1000 K within 30 ps, using a 1 fs timestep. In this stage of the calculation the force constants for the non-bonded interactions and the angle energy constant for the diastereospecifically unassigned groups were gradually increased to their final values. In the next stage of the calculation the system was cooled from 1000 K to 100 K within 15 ps (1 fs timestep), applying the high force constants obtained at the end of the previous cooling stage. In order to detect the

energy minimum, 200 steps of energy minimization were performed, using the Powell algorithm (Powell, 1977).

Of the 120 structures resulting from the final round of structure calculation, those 80 structures that showed the lowest energy and the least violation of the experimental data were selected for further characterization. All calculations were carried out on Sun SparcUltra workstations requiring an average of 45 minutes of cpu time for each calculated structure. The coordinates were deposited in the Protein Data Bank, Brookhaven National Laboratory, Upton, NY, with the code 2FN2.

Geometry of the structures and elements of secondary structure were analyzed using PROCHECK (Laskowski *et al.*, 1993). For the graphical presentation of the structures the programs SYBYL 6.0 (Tripos Ass.), INSIGHT 2.3 (Biosym Inc.), MOLSCRIPT (Kraulis, 1991) and Raster3D (Bacon & Anderson, 1988; Merritt & Murphy, 1994) were used.

Generation of a model for the ^{1}F2^{2}F2 module pair

Models of the ^{1}F2^{2}F2 module pair were generated within X-PLOR by covalently linking the minimized average structures of ^{1}F2 and ^{2}F2, and randomizing those inter-module backbone dihedral angels that were found to be disordered in the individual modules. In addition, the preliminary structure of the ^{6}F1^{1}F2 module pair (A. Bocquier, personal communication) was used for a further reduction of the conformational space accessible for a ^{1}F2^{2}F2 module pair. The resulting structures were energy minimized in 200 steps of conjugate gradient minimization (Powell, 1977) using the full CHARMM potential function (Brooks *et al.*, 1983). Structures that showed favourable non-covalent inter-module interactions were selected for further characterization.

The arrangement of the putative collagen binding sites was deduced by measuring the distances and relative orientation between the single tryptophan residues of the two modules. The resonances of the corresponding tryptophan in PDC-109b were the most sensitive to ligand binding in an NMR-monitored study (Constantine *et al.*, 1992).

Acknowledgements

This is a contribution from the Oxford Centre of Molecular Sciences which is supported by the BBSRC, EPSRC and MRC. H. S. was supported by a Deutsche Forschungsgemeinschaft Fellowship; A. R. P. and J. R. P. thank the Wellcome Trust for financial support. We thank Tony Willis, Robin Aplin, Armin Metzger and Graeme Shaw for their help and advice concerning N-terminal sequencing, mass spectrometry and NMR spectroscopy.

References

Allan, J. A., Docherty, A. J. P., Barker, P. J., Huskisson, N. S., Reynolds, J. J. & Murphy, G. (1995). Binding of gelatinases A and B to type-I collagen and other matrix components. *Biochem. J.* **309**, 299–306.

Bacon, D. J. & Anderson, W. F. (1988). A fast algorithm for rendering space-filling molecule pictures. *J. Mol. Graphics,* **6**, 219–220.

Banyai, L. & Patthy, L. (1991). Evidence for the involvement of type II domains in collagen binding by 72 kDa type IV procollagenase. *FEBS Letters,* **282**, 23–25.

Banyai, L., Tordai, H. & Patthy, L. (1994). The gelatin-binding site of human type IV collagenase (gelatinase A). *Biochem. J.* **298**, 403–407.

Banyai, L., Tordai, H. & Patthy, L. (1996). Structure and domain-domain interactions of the gelatin-binding site of human 72-kilodalton type IV collagenase (gelatinase A, matrix metalloproteinase 2). *J. Biol. Chem.* **271**, 12003–12008.

Berendsen, H. J. C., Postma, J. P. M., van Gunsteren, W. F., DiNiola, A. & Haak, J. R. (1984). Molecular dynamics with coupling to an external bath. *J. Chem. Phys.* **81**, 3684–3690.

Bernard, B. A., Yamada, K. M. & Olden, K. (1982). Carbohydrates selectively protect a specific domain of fibronectin against proteases. *J. Biol. Chem.* **257**, 8549–8554.

Brooks, B. R., Bruccoleri, R. E., Olafson, B. D., States, D. J., Swaminathan, S. & Karplus, M. (1983). CHARMM: a program for macromolecular energy, minimization and dynamics calculations. *J. Comput. Chem.* **4**, 187–217.

Brown, S. C., Weber, P. L. & Mueller, L. (1988). Toward complete ^{1}H NMR spectra in proteins. *J. Magn. Reson.* **77**, 166–169.

Brünger, A. T. (1993). *X-PLOR Version 3.1,* Howard Hughes Institute & Yale University, New Haven, CT.

Brünger, A. T., Clore, G. M., Gronenborn, A. M. & Karplus, M. (1986). Three-dimensional structure of proteins determined by molecular dynamics with interproton distance restraints: application to crambin. *Proc. Natl Acad. Sci. USA,* **83**, 3801–3805.

Collier, I. E., Krasnov, P. A., Strongin, A. Y., Birkedal-Hansen, H. & Goldberg, G. I. (1992). Alanine scanning mutagenesis and functional analysis of the fibronectin-like collagen-binding domain from human 92-kDa type IV collagenase. *J. Biol. Chem.* **267**, 6776–6781.

Constantine, K. L., Ramesh, V., Banyai, L., Trexler, M., Patthy, L. & Llinas, M. (1991). Sequence-specific ^{1}H NMR assignments and structural characterization of bovine seminal fluid protein PDC-109 domain b. *Biochemistry,* **30**, 1663–1672.

Constantine, K. L., Madrid, M., Banyai, L., Trexler, M., Patthy, L. & Llinas, M. (1992). Refined solution structure and ligand-binding properties of PDC-109 domain b, a collagen-binding type II domain. *J. Mol. Biol.* **223**, 281–298.

Davis, D. G. & Bax, A. (1985). Assignment of complex ^{1}H NMR spectra via two-dimensional homonuclear Hartmann-Hahn spectroscopy. *J. Am. Chem. Soc.* **107**, 2820–2821.

Davis, J. T., Hirani, S., Bartlett, C. & Reid, B. R. (1994). ^{1}H NMR studies on an Asn-linked glycopeptide. GlcNAc-1 C2-N2 bond is rigid in H_2O. *J. Biol. Chem.* **269**, 3331–3338.

Deisenhofer, J. (1981). Crystallographic refinement and atomic models of a human Fc fragment and its complex with fragment B of protein A from *Staphylococcus aureus* at 2.9 Å and 2.8 Å resolution. *Biochemistry,* **20**, 2361–2370.

Dellanoy, P. & Montreuil, J. (1989). Deglycosylation of the chymotryptic collagen-binding fragment of human plasma fibronectin does not modify its affinity to denatured collagen. *FEBS Letters,* **247**, 25–27.

Eberle, W., Pastore, A., Sander, C. & Rösch, P. (1991). The structure of ColE1 rop in solution. *J. Biomol. NMR,* **1**, 71–82.

Fletcher, C. M., Harrison, R. A., Lachmann, P. J. & Neuhaus, D. (1994). Structure of a soluble, glycosylated form of the human complement regulatory protein CD59. *Structure,* **2**, 185–199.

Forastieri, H. & Ingham, K. C. (1985). Interaction of gelatin with a fluorescein-labeled 42-kDa chymotryptic fragment of fibronectin. *J. Biol. Chem.* **260**, 10546–10550.

Guidry, C., Miller, E. J. & Hook, M. (1990). A second fibronectin-binding region in collagen α chains. *J. Biol. Chem.* **265**, 19230–19236.

Hahn, L. & Yamada, K. (1979). Identification and isolation of a collagen-binding fragment of the adhesive glycoprotein fibronectin. *Proc. Natl. Acad. Sci. USA,* **76**, 1160–1163.

Holak, T. A., Nilges, M. & Oschkinat, H. (1989). Improved strategies for the determination of protein structures from NMR data: the solution structure of acyl carrier protein. *FEBS Letters,* **242**, 649–654.

Hyberts, S. G., Goldberg, M. S., Havel, T. F. & Wagner, G. (1992). The solution structure of eglin c based on measurements of many NOEs and coupling constants and its comparison with X-ray structures. *Protein Sci.* **1**, 736–751.

Hynes, R. O. (1990). *Fibronectins,* Springer-Verlag, Berlin.

Imberty, A. & Pérez, S. (1995). Stereochemistry of the N-glycosylation sites in glycoproteins. *Protein Eng.* **8**, 699–709.

Imberty, A., Bourne, Y., Cambillau, C., Rougé, P. & Pérez, S. (1993). Oligosaccharide conformation in protein carbohydrate complexes. *Advan. Biophys. Chem.* **3**, 71–117.

Ingham, K. C., Brew, S. A. & Migliorini, M. M. (1989). Further localization of the gelatin-binding determinants within fibronectin. *J. Biol. Chem.* **264**, 16977–16980.

Ingham, K. C., Brew, S. A. & Novokhatry, V. V. (1995). Influence of carbohydrate on structure, stability, and function of gelatin-binding fragments of fibronectin. *Arch. Biochem. Biophys.* **316**, 235–240.

Jones, G. E., Arumugham, R. G. & Tanzer, M. L. (1976). Fibronectin glycosylation modulates fibroblast adhesion and cell spreading. *J. Cell. Biol.* **103**, 1663–1670.

Kemmink, J., Darby, N. J., Dijkstra, K., Nilges, M. & Creighton, T. E. (1996). Structure determination of the N-terminal thioredoxin-like domain of protein disulfide isomerase using multidimensional heteronuclear ^{13}C/^{15}N NMR spectroscopy. *Biochemistry,* **35**, 7684–7691.

Kessler, H., Matter, H., Gemmecker, G., Kling, A. & Kottenhahn, M. (1991). Solution structure of a synthetic N-glycosylated cyclic hexapeptide determined by NMR spectroscopy and MD calculations. *J. Am. Chem. Soc.* **113**, 7550–7563.

Kharrat, A., Macias, M. J., Gibson, T. J., Nilges, M. & Pastore, A. (1995). Structure of the dsRNA binding domain of *E.coli* RNase III. *EMBO J.* **14**, 3572–3584.

Kottgen, E., Hell, B., Muller, C., Kainer, F. & Tauber, R. (1989). Developmental changes in the glycosylation and binding properties of human fibronectins. Characterization of the glycan structures and ligand binding of human fibronectins from adult plasma, cord blood and amniotic fluid. *Biol. Chem.* **370**, 1285–1294.

Kraulis, P. J., Clore, G. M., Nilges, M., Jones, T. A., Petterson, G., Knowles, J. & Gronenborn, A. M. (1989). Determination of the three-dimensional solution structure of the C-terminal domain of cellobiohydrolase I from *Trichoderma reesei*. A study using nuclear magnetic resonance and hybrid distance geometry-dynamical simulated annealing. *Biochemistry,* **28**, 7241–7257.

Kraulis, P. K. (1991). MOLSCRIPT: a program to produce both detailed and schematic plots of protein structures. *J. Appl. Crystallog.* **24**, 946–950.

Krusius, T., Fukuda, M., Dell, A. & Rusolahti, E. (1985). Structure of the carbohydrate units of human amniotic fluid fibronectin. *J. Biol. Chem.* **260**, 4110–4116.

Kumar, A., Ernst, R. R. & Wüthrich, K. (1980). A two-dimensional nuclear Overhauser enhancement (2D NOE) experiment for elucidation of complete proton-proton cross-relaxation networks in biological macromolecules. *Biochem. Biophys. Res. Commun,,* **95**, 1–6.

Laskowski, R. A., MacArthur, M. W., Moss, D. S. & Thornton, J. M. (1993). PROCHECK: a program to check the stereochemical quality of protein structures. *J. Appl. Crystallog.* **26**, 283–291.

Litvinovich, S. V., Strickland, D. K., Medved, L. V. & Ingham, K. C. (1991). Domain structure and interactions of the type I and type II modules in the gelatin-binding region of fibronectin. *J. Mol. Biol.* **217**, 563–575.

Malhotra, R., Wormald, M. W., Rudd, P. M., Fisher, P. B., Dwek, R. A. & Sim, R. B. (1995). Glycosylation changes of IgG associated with rheumatoid arthritis can activate complement via the mannose-binding protein. *Nature Med.* **1**, 237–243.

Marion, D., Ikura, M., Tschudin, R. & Bax, A. (1989). Rapid recording of 2D NMR spectra without phase cycling. Application to the study of hydrogen exchange in proteins. *J. Magn. Reson.* **85**, 393–399.

Merritt, E. A. & Murphy, M. (1994). Raster3D version 2.0 – a program for photorealistic molecular graphics. *Acta Crystallog. sect D,* **50**, 869–873.

Morton, C. J., Pugh, D. J. R., Brown, E. L. J., Kahmann, J. D., Renzoni, D. A. C. & Campbell, I. D. (1996). Solution structure and peptide binding of the SH3 domain from human Fyn. *Structure,* **4**, 705–714.

Mueller, L. (1987). P. E. COSY, a simple alternative to E. COSY. *J. Magn. Reson.* **72**, 191–196.

Murphy, G., Ngyen, Q., Cockett, M. I., Atkinson, S. J., Allan, J. A., Knight, C. G., Willenbrock, F. & Docherty, A. J. P. (1994). Assessment of the role of the fibronectin-like domain of gelatinase A by analysis of a deletion mutant. *J. Biol. Chem.* **269**, 6632–6636.

Nilges, M. (1993). A calculation strategy for the structure determination of symmetric dimers by ^{1}H NMR. *Proteins: Struct. Funct. Genet.* **17**, 297–309.

Pickford, A. R., Potts, J. R., Bright, J. R., Phan, I. & Campbell, I. D. (1997). Solution structure of a type 2 module from fibronectin: implications for the structure and function of the gelatin-binding domain. *Structure,* **5**, 359–370.

Potts, J. R. & Campbell, I. D. (1994). Fibronectin structure and assembly. *Curr. Opin. Cell. Biol.* **6**, 648–655.

Potts, J. R. & Campbell, I. D. (1996). Structure and function of fibronectin modules. *Matrix Biol.* **15**, 313–320.

Powell, M. J. D. (1977). Restart procedures for the conjugate gradient method. *Math. Prog.* **12**, 241–254.

Rance, M., Sørensen, O. W., Bodenhausen, G., Wagner, G., Ernst, R. R. & Wüthrich, K. (1983). Improved spectral resolution in COSY ^{1}H NMR spectra of proteins via a double quantum filter. *Biochem. Biophys. Res. Commun.* **117**, 479–485.

Vliegenthart, J. F. G., Dorland, L. & van Haleek, H. (1983). High-resolution ^{1}H-nuclear magnetic resonance spectroscopy as a tool in the structural analysis of carbohydrates related to glycoproteins. *Advan. Carbohyd. Chem. Biochem.* **41**, 209–374.

Weis, W. I., Brünger, A. T., Skehel, J. J. & Wiley, D. C. (1990). Refinement of the influenza virus hemagglutinin by simulated annealing. *J. Mol. Biol.* **212**, 737–761.

Williams, M. J., Phan, I., Baron, M., Driscoll, P. C. & Campbell, I. D. (1993). Secondary structure of a pair of fibronectin type l modules by two-dimensional nuclear magnetic resonance. *Biochemistry,* **32**, 7388–7395.

Wishart, D. S., Sykes, B. D. & Richards, F. M. (1992). The chemical shift index: a fast and simple method for the assignment of protein secondary structure through NMR spectroscopy. *Biochemistry,* **31**, 1647–1651.

Wormald, M. R., Wooten, E. W., Bazzo, R., Edge, C. J., Feinstein, A., Rademacher, T. W. & Dwek, R. A. (1991). The conformational effects of N-glycosylation on the tailpiece from serum IgM. *Eur. J. Biochem.* **198**, 131–139.

Wüthrich, K. (1986). *NMR of Proteins and Nucleic Acids,* John Wiley & Sons, New York.

Wyss, D. F., Choi, J. S., Li, J., Knoppers, M. H., Willis, K. J., Arulanandam, A. R. N., Smolyer, A., Reinherz, E. L. & Wagner, G. (1995). Conformation and function of the N-linked glycan in the adhesion domain of human CD2. *Science,* **269**, 1273–1276.

Zhu, B. C. R. & Laine, R. A. (1985). Polylactosamine glycosylation on human fetal placental fibronectin weakens the binding affinity of fibronectin to gelatin. *J. Biol. Chem.* **260**, 4041–4045.

Zhu, B. C. R., Laine, R. A. & Barkley, M. D. (1990). Intrinsic tryptophan fluorescence measurements suggest that polyactosamine glycosylation affects the protein conformation of the gelatin-binding domain from human placental fibronectin. *Eur. J. Biochem.* **189**, 509–516.

Edited by P. E. Wright

(Received 12 August 1997; received in revised form 24 October 1997; accepted 5 November 1997)

http://www.hbuk.co.uk/jmb

Supplementary material for this paper comprising one Table is available from JMB Online.